Cell Death and Differentiation (2007) 14, 1792–1801

www.nature.com/cdd

Activation of PKA and phosphorylation of sodium-dependent vitamin C transporter 2 by prostaglandin E2 promote osteoblast-like differentiation in MC3T3-E1 cells

X Wu[1,2], L-H Zeng[3], T Taniguchi[2] and Q-M Xie*[,1]

Sodium-dependent vitamin C transporter (SVCT) 2-mediated L-ascorbic acid (AA) uptake is required in osteoblast-like differentiation of MC3T3-E1 cells, and prostaglandin E2 (PGE2) is among the most important local factors in bone formation, but the detailed mechanism by which PGE2 induces osteoblast differentiation remains obscure. We revealed that PGE2 induced AA uptake and osteoblast-like differential markers including alkaline phosphatase, collagen, osteocalcin expression, and mineralization in MC3T3-E1 cells. Inhibition of AA uptake by SVCT2 short isoform functioning as a dominant-negative mutant not only robustly attenuated PGE2-induced markers expression and mineralization, but also decreased their basal levels. However, upregulation of AA uptake resulted from PGE2-induced plasma membrane translocation of cytoplasm SVCT2, and this effect was abolished by pretreatment with EP4 receptor antagonist, AH-23848B or cAMP-dependent protein kinase A (PKA) inhibitor, H-89. Moreover, we showed SVCT2 physically interacted with PKA in immunoprecipitates, and PKA phosphorylated SVCT2 *in vitro* and in intact cells at Ser402 and Ser639 sites; however, mutation of Ser402 or/and Ser639 in SVCT2 severely diminished SVCT2 translocation in response to PGE2. Together, these results suggest that PGE2-induced SVCT2 plasma membrane translocation through EP4 receptor and subsequent phosphorylation of SVCT2 at Ser402 and Ser639 sites by PKA results in an increase of AA uptake and consequent promotion of osteoblast-like differentiation in MC3T3-E1 cells.
Cell Death and Differentiation (2007) **14,** 1792–1801; doi:10.1038/sj.cdd.4402190; published online 22 June 2007

MC3T3-E1 preosteoblast, an osteoblastic cell line derived from normal mouse calvaria expresses osteoblast-like differential markers and forms mineralized extracellular matrix only after exposure to L-ascorbic acid (reduced vitamin C, AA).[1,2] AA stimulates procollagen hydroxylation, processing, and fibril assembly followed by the dramatic induction of specific genes associated with the osteoblastic phenotype, including alkaline phosphatase (ALP), osteopontin, and osteocalcin (OCN).[3,4] Sodium-dependent vitamin C transporters 1 and 2 (SVCT1, 2) facilitate the transport of AA,[5–7] and sodium-dependent AA transport is required for MC3T3-E1 cells to achieve the millimolar intracellular AA concentration that is necessary for maximal prolyl hydroxylase activity and expression of the osteoblast phenotype.[8] We had demonstrated that SVCT2 instead of SVCT1 is expressed in MC3T3-E1 cells,[9] Ca^{2+}, PO_4^{3-}, or Zn^{2+} enhances osteoblast-like differentiation through increase of SVCT2 expression and AA uptake,[10,11] and SVCT2 overexpression in MC3T3-E1 cells stimulates mineralization and promotes differential marker genes expression.[12] Additionally, in SVCT2-deficient mouse, AA level was undetectable or markedly reduced in the blood and tissues, and the SVCT2-deficient mice died within a few minutes of birth due to respiratory failure and intraparenchymal brain hemorrhage, suggesting that SVCT2 is required for transport of AA into many tissues and plays an important role in the development of mouse.[7]

Prostaglandins (PGs) are produced both in skeletal tissue and bone cell culture in response to various stimulus, and are among the most important local factors with autocrine/paracrine roles in bone.[13] Among the various PGs produced in bone tissue, the most abundant one is prostaglandin E2 (PGE2), and it appears to be of utmost importance in bone physiology. Although PGE2 is initially described as a potent bone-resorbing substance,[14,15] accumulated evidence indicates that PGE2 is a potent stimulator of bone formation *in vivo* and *in vitro*.[16–20] It was reported that PGE2 induced ALP activity and increased collagen protein synthesis in MC3T3-E1 cells,[21,22] and continuous exposure of fetal rat calvaria cells to PGE2 induced a significant increase in mineralized bone nodule formation.[23,24] However, the detailed mechanism by which PGE2 induces osteoblast differentiation remains obscure.

In this study, we suggest that PGE2 induces plasma membrane localization of cytoplasm SVCT2 through EP4

[1]Zhejiang Respiratory Drugs Research Laboratory of State Foods and Drugs Administration of China, Medical School of Zhejiang University, Hangzhou 310058, China; [2]Department of Toxicology, Graduate School of Pharmaceutical Sciences, Osaka University, Osaka 565-0871, Japan and [3]Department of Pharmacology, Medical School of Zhejiang University, Hangzhou 310058, China
*Corresponding author: Professor Q-M Xie, Zhejiang Respiratory Drugs Research Laboratory of State Foods and Drugs Administration of China, Medical School of Zhejiang University, No.388 Yuhangtang Road, Hangzhou 310058, China. Tel: +86 571 8820 8231; Fax: +86 571 8820 8231; E-mail: xieqm@zju.edu.cn
Keywords: prostaglandin E2; PKA; sodium-dependent vitamin C transporter; osteoblast-like differentiation
Abbreviations: SVCT2, sodium-dependent vitamin C transporter 2; PGE2, prostaglandin E2; PKA, cAMP-dependent protein kinase A; AA, L-ascorbic acid; ALP, alkaline phosphatase; Hyp, hydroxyproline; OCN, osteocalcin; dnSVCT2, SVCT2 short isoform
Received 11.12.06; revised 10.5.07; accepted 28.5.07; Edited by G Cossu; published online 22.6.07

receptor and phosphorylation of SVCT2 at Ser402 and Ser639 sites by cAMP-dependent protein kinase A (PKA), followed by an increase of AA transport into cells, which consequently leads to stimulation of osteoblast-like differentiation in MC3T3-E1 cells.

Results

PGE2 induces osteoblast-like differentiation and AA uptake. To assess the effects of PGE2 on osteoblast-like differentiation in MC3T3-E1 cells, we performed long-term cultures and analysis of early-stage differential markers including ALP, collagen, and late-stage non-collagenous bone matrix marker, OCN expression as well as mineralization in MC3T3-E1 cells. Cells treated with vehicle underwent robustly osteoblast-like differentiation exhibiting time-dependent increases in ALP, collagen-specific hydroxyproline (Hyp), OCN levels, and mineralization (Figure 1). However, 1 μM of PGE2 treatment for different times consistently increased ALP activity and Hyp contents by 2- to 3-fold over the vehicle treatment at all time points (Figure 1a and b), and PGE2 from 1 nM to 1 μM dose-dependently induced ALP and Hyp levels as well as ALP and α(I)procollagen mRNA expression in confluent cells (Supplementary Figure S1A and B). Moreover, PGE2 treatment for different times robustly stimulated OCN expression and formation of von-Kossa stainable mineralized nodules over vehicle treatment at all time points (Figure 1c and d).

To determine whether PGE2 induces AA uptake, cells were treated with 1 μM of PGE2 for 1 h, and then subjected to [l-^{14}C]AA uptake, the kinetic parameters including K_m and V_{max} were applied to assess the effects of PGE2. PGE2 increased the V_{max} values of AA uptake by approximately threefold over the vehicle, whereas it did not obviously change the K_m values of AA uptake (Figure 1e and f). Similarly, long-term cultures of primary calvarial osteoblasts indicated 1 μM of PGE2 treatment for different times also robustly induced AA uptake, and significantly increased osteoblast differential markers including ALP, Hyp, and OCN expression as well as mineralization (Supplementary Figure S3A–F). Together, PGE2 stimulates osteogenic markers expression as well as mineralization in MC3T3-E1 cells and primary calvarial osteoblasts, and PGE2 induces AA uptake with increases of V_{max} and no change in K_m values.

SVCT2 and AA uptake are required in PGE2-induced osteoblast-like differentiation. Human SVCT2 short isoform (dnSVCT2) functions as a dominant-negative inhibitor in AA uptake,[25] we attempted to clone the mouse dnSVCT2 cDNA and generated dnSVCT2-expressing retrovirus to examine whether SVCT2 and AA uptake mediate PGE2-induced osteoblast-like differentiation in MC3T3-E1 cells. Overexpression of dnSVCT2 in cells infected with dnSVCT2-expressing retrovirus was verified by Western blotting, and the effect of dnSVCT2 on AA uptake was assessed by kinetic parameters. Expression of dnSVCT2 led to approximately 8-fold increases of dnSVCT2 without change of endogenous SVCT2 levels in whole cell lysates (Figure 2a); however, no obvious

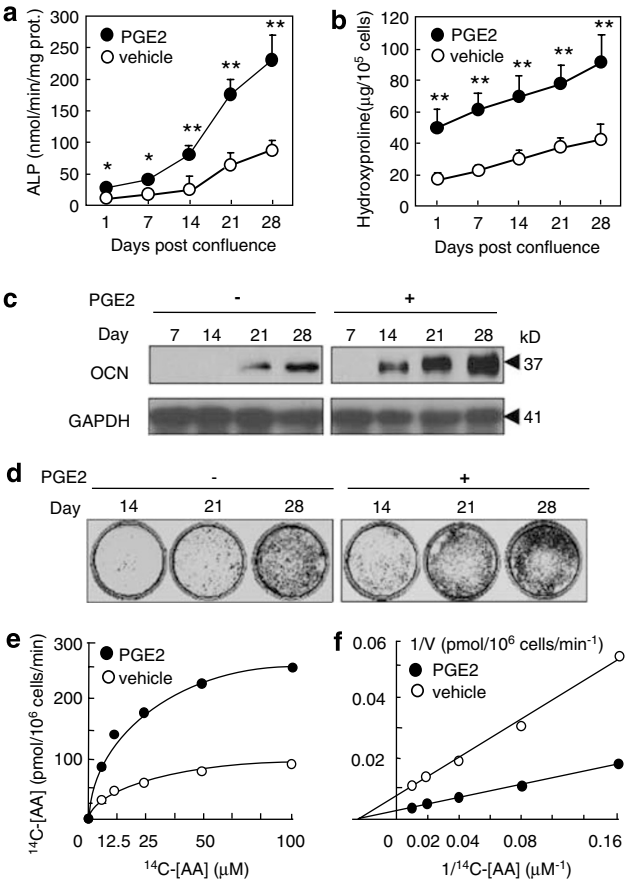

Figure 1 PGE2 induces osteoblast-like differentiation and [l-^{14}C]AA uptake in MC3T3-E1 cells. Twenty four hours after plated, cells were precultured in serum-free αMEM containing 1 μg/ml of indomethacin for 3 h, and further treated along with 1 μM of PGE2 (+) or vehicle (−) for indicated times (**a–d**) or 1 h (**e**, and **f**). Then, cells were harvested for ALP activity (**a**) and Hyp contents (**b**) assays, Western blotting assays for OCN expression (**c**), von Kosa staining, (**d**) and AA uptake assays by using different concentrations of [l-^{14}C]AA (**e**, and **f**). Numerical data were expressed as mean ± S.D. from at least three independent cultures, $^*P<0.05$; $^{**}P<0.01$ *versus* vehicle-treated cells. Kinetic constants of AA uptake, K_m and V_{max}, were calculated by fitting the data to a double reciprocal plot, and expressed as μM, and pmol/10^6 cells/min respectively

difference in K_m values of AA uptake was observed between cells expressing either control EGFP or dnSVCT2, whereas dnSVCT2 did decrease the V_{max} values to approximately 39% of control EGFP (Figure 2b and c).

PGE2 stimulating AA uptake as well as osteoblast-like differentiation in MC3T3-E1 cells prompted us to hypothesize that SVCT2-mediated AA uptake is required in PGE2-induced osteoblast-like differentiation. Similarly, we performed long-term cultures and analysis of ALP, collagen, and OCN expression as well as mineralization in MC3T3-E1 cells infected with either control EGFP- or dnSVCT2-expressing viruses, followed by stimulation with PGE2 for different times. Infection with either EGFP or dnSVCT2 expression retrovirus did not markedly affect the cell proliferation and cell morphology, and PGE2 treatment for different times in EGFP-expressing cells significantly stimulated ALP, collagen, and OCN expression as well as mineralization at all time points, whereas overexpression of dnSVCT2 not only

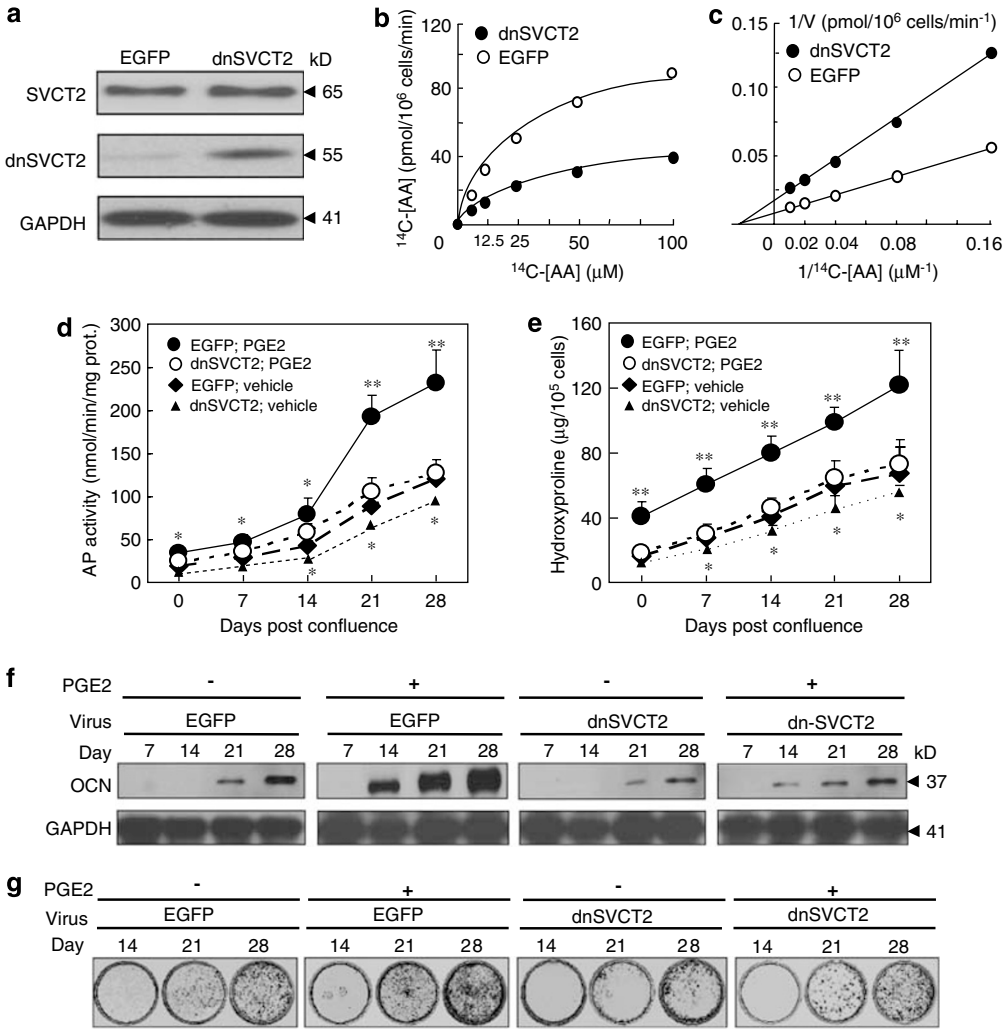

Figure 2 SVCT2 and AA uptake mediate PGE2-induced osteoblast-like differentiation in MC3T3-E1 cells. MC3T3-E1 cells were infected with dnSVCT2 or EGFP expression retrovirus for 24 h, then, cells were either harvested for Western blotting assay for dnSVCT2 expression (**a**), uptake assay by using different concentrations of [l-^{14}C]AA (**b,** and **c**) or precultured in serum-free αMEM containing 1 μg/ml of indomethacin for 3 h, and further treated along with PGE2 (+) or vehicle (−) for indicated times. After PGE2 treatment, cells were harvested for ALP activity (**d**) and Hyp contents (**e**) assays, Western blotting for OCN expression (**f**), von Kosa staining (**g**). Numerical data were expressed as mean ± S.D. from at least three independent cultures, *$P<0.05$; **$P<0.01$ *versus* vehicle-treated and EGFP virus-infected cells. Kinetic constants of AA uptake, K_m and V_{max}, were calculated by fitting the data to a double reciprocal plot, and expressed as μM and pmol/10^6 cells/min, respectively

significantly inhibited PGE2-induced osteogenic markers expression and mineralization, but also decreased their basal levels at all time points (Figure 2d–g). Together, dnSVCT2 functioning as a dominant inhibitor for AA uptake in MC3T3-E1 cells not only robustly inhibited PGE2-induced osteoblast-like differential markers expression and mineralization, but also significantly decreased their basal levels.

Membrane localization of SVCT2 results in PGE2-induced AA uptake. To determine the mechanism by which PGE2 induces AA uptake, SVCT2 expression levels in whole cells and subcellular fractions in response to PGE2 were examined. Although 1 μM of PGE2 treatment for 1 h robustly increased AA uptake (Figure 1e and f), both Northern blotting and Western blotting assays suggested that PGE2 treatment within 1 h did not obviously induce SVCT2 mRNA and protein expression (Figure 3a and b). Subcellular distribution of SVCT2 was further examined by Western blotting, and results revealed that PGE2 robustly increased plasma membrane SVCT2 levels, and concurrently decreased cytoplasm SVCT2 levels in time- and dose-dependent manners (Figure 3c and e), consistent with the results from uptake assays indicating that PGE2 time- and dose-dependently stimulated AA uptake in MC3T3-E1 cells (Figure 3d and f). Moreover, immunostaining for endogenous SVCT2 protein further indicated that in unstimulated cells, SVCT2 was mainly distributed diffusely in the cytoplasm (Figure 4g), however, 1 h after PGE2 stimulation, SVCT2 molecule was largely translocated to the plasma membrane in a punctuate pattern (Figure 4h). This effect was further confirmed in primary calvarial osteoblast cultures, indicating that PGE2 time-dependently induced SVCT2 plasma membrane localization and concurrently decreased the accumulation of SVCT2 in cytoplasm, as a

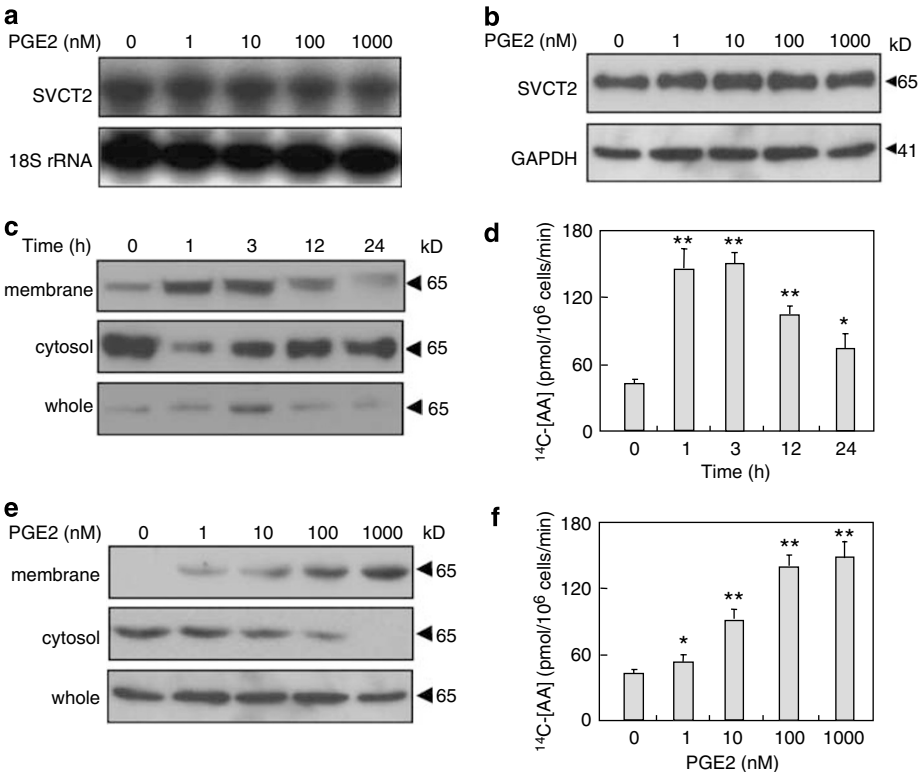

Figure 3 PGE2 stimulates SVCT2 plasma membrane translocation and AA uptake in MC3T3-E1 cells. For dose-dependent effects (**a, b, e,** and **f**), MC3T3-E1 cells were precultured in serum-free αMEM containing 1 μg/ml of indomethacin for 3 h, and further treated along with indicated concentrations of PGE2 for 1 h, and then, cells were harvested for determination of SVCT2 mRNA expression (**a**) by Northern blotting, SVCT2 protein levels in whole cells (**b**) or subcellular fractions (**e**) by Western blotting and AA uptake (**f**) by using 25 μM of [l-^{14}C]AA. For time-dependent effects, MC3T3-E1 cells were precultured in serum-free αMEM containing 1 μg/ml of indomethacin for 3 h, and further treated along with 1000 nM of PGE2 for indicated times, then, cells were harvested for determination of SVCT2 protein levels in subcellular fractions (**c**) by Western blotting assays and AA uptake by using 25 μM of [l-^{14}C]AA (**d**). Experiments were independently triplicated, and results were qualitatively identical. Representative experiments are shown. Numerical data were expressed as mean $\pm$ S.D. from at least three independent cultures, $^*P<0.05$; $^{**}P<0.01$ *versus* either 0 h treatment or 0 nM of PGE2 treatment, respectively

result, PGE2 time-dependently increased AA uptake in primary calvarial osteoblasts too (Supplementary Figure S3G and H). Together, SVCT2 plasma membrane localization instead of upregulation of SVCT2 mRNA and protein expression in response to PGE2 results in stimulation of AA uptake.

EP4 receptor and PKA activation are required in SVCT2 translocation. PGE2 acts through at least four subtypes of rhodopsin-type G protein-coupled receptors, named EPs: EP1 raises intracellular Ca^{2+} concentration, EP2, and EP4 simulate adenylate cyclase (AC), and EP3 decreases intracellular cAMP concentration.[26] EP2 and EP3 mRNA expression was not detectable in MC3T3-E1 cells even with 15 μg poly(A)$^+$ RNA in Northern blotting, only EP1 and EP4 are expressed in MC3T3-E1 cells.[27] To determine which EP receptor subtypes were involved in PGE2-induced SVCT2 translocation and osteoblast-like differentiation, selective EP1 or EP4 receptor antagonist, either AH-6809 or AH-23848B was applied for pretreatment in MC3T3-E1 cells, followed by stimulation with 1 μM of PGE2. AH-23848B instead of AH-6809 dose-dependently inhibited SVCT2 plasma membrane localization and concurrently increased the accumulation of SVCT2 in cytoplasm of PGE2-treated cells, and 10 μM of AH-23848B almost completely abrogated PGE2-induced plasma membrane localization of SVCT2 (Figure 4a and b). Consistent with these results, AH-23848B but not AH-6809 dose-dependently inhibited AA uptake in response to PGE2, and 10 μM of AH-23848B almost completely diminished PGE2-induced AA uptake (Figure 4d and e). Similarly, immunostaining results revealed that within 1 h, SVCT2 molecule was largely translocated to the plasma membrane in a punctuate pattern in response to PGE2 (Figure 4g and h), however, 10 μM of AH-23838B but not AH-6809 markedly attenuated PGE2-induced plasma membrane accumulation of SVCT2 (Figure 4i and j). Consistent with the effects of AH-23848B on subcellular distribution of SVCT2 and AA uptake, AH-23848B instead of AH-6809 significantly inhibited PGE2-induced ALP activity as well as Hyp contents in a dose-dependent manner (Supplementary Figure S2a and b).

Activation of EP4 receptor simulates AC, and subsequently increases intracellular cAMP concentration, which further leads to increases of PKA activity.[26] To test whether this signaling cascade is involved in PGE2-induced SVCT2 plasma membrane localization and AA uptake, we examined the cAMP levels and PKA activity in MC3T3-E1 cells treated with PGE2 by ELISA and Western blotting assays,

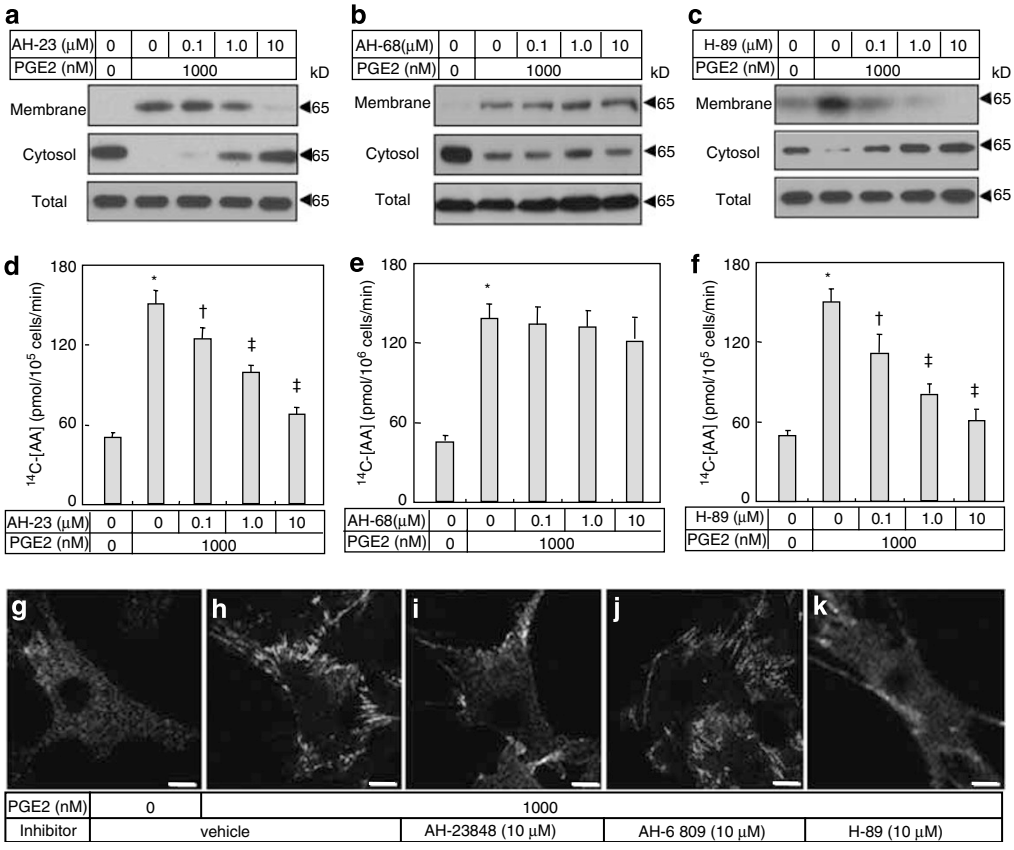

Figure 4 Effects of various inhibitors including AH-23848B, AH-6809, and H-89 on PGE2-induced SVCT2 translocation, AA uptake. MC3T3-E1 cells were previously treated with indicated concentrations of inhibitors and 1 μg/ml of indomethacin in serum-free αMEM for 3 h, and further treated along with 1000 nM of PGE2 for additional 1 h. After that, cells were harvested for detection of SVCT2 subcellular localization in cytoplasm and plasma membrane (**a–c**) by Western blotting, AA uptake assay by using 25 μM of [l-^{14}C]AA (**d–f**), or immunostaining (**g–k**) with rabbit anti-SVCT2 first antibody and anti-rabbit Alex555-conjugated second antibody (bars, 100 μm). Numerical data were expressed as mean $\pm$ S.D. from at least three independent culture, $^{*}P<0.01$ *versus* absence of inhibitor and PGE2; $^{\dagger}P<0.05$, $^{\ddagger}P<0.01$ *versus* PGE2 treated cells in the absence of inhibitor

respectively. PGE2 dose-dependently increased intracellular cAMP contents (Supplementary Figure S2C), and robustly activated PKA (Figure 5a). Moreover, pretreatment of cells with PKA inhibitor, H-89, not only dose-dependently inhibited the accumulation of SVCT2 in plasma membrane but also concurrently increased SVCT2 in cytoplasm in response to PGE2 (Figure 4c), which is consistent with the results from uptake assay and immunostaining indicating that H-89 dose-dependently attenuated PGE2-induced AA uptake (Figure 4f) and H-89 at 10 μM almost completely ablated PGE2-induced SVCT2 plasma membrane accumulation (Figure 4k). Moreover, H-89 significantly inhibited PGE2-induced ALP activity as well as Hyp contents in a dose-dependent manner (Supplementary Figure S2D). Overall, these data indicate that PGE2 stimulates SVCT2 plasma membrane localization and AA uptake through a signaling cascade involving EP4-AC-cAMP-PKA.

PKA phosphorylates SVCT2 at Ser402 and Ser639 sites. To examine the likely physical interaction between PKA and SVCT2, we performed co-immunoprecipitation using whole cell lysates with anti-catalytic PKA unit (cPKA) or anti-SVCT2 antibodies. Protein complexes in the immunoprecipitates were detected by Western blotting with the indicated antibodies (Figure 5a). The protein complexes from either vehicle- or PGE2-treated cells precipitated with a SVCT2 antibody containing cPKA in addition to SVCT2 as expected, and the complexes from PGE2-treated but not vehicle-treated cells precipitated with a cPKA antibody containing SVCT2 in addition to cPKA as expected; however, precipitates from the control IgG, on the other hand, did not contain any proteins (Figure 5a).

To determine the functional consequences of physical interaction between cPKA and SVCT2, we analyzed the primary structure of mSVCT2, finding that two putative PKA phosphorylation sites (Ser402 and Ser639) located in C-terminal (Figure 5b). To assess their potential importance, we expressed myc-tagged wild type of SVCT2 (WT) and SVCT2 variants that harbored mutations at the serine residues (Ser to Ala) individually (S402A, S639A) or in combination (S402/639A), and performed *in vitro* phosphorylation assays by using purified active PKA catalytic unit, followed by sodium dodecyl sulfate-polyacrylamide gel electrophoresis (SDS-PAGE) and autoradiography. The wild-type SVCT2 incorporated robust levels of ^{32}P, whereas both S402A and S639A showed marked reduction, as expected, the double mutant, S402/639A incorporated no ^{32}P (Figure 5c). Western blotting using the myc antibody further confirmed that the ^{32}P-labeled

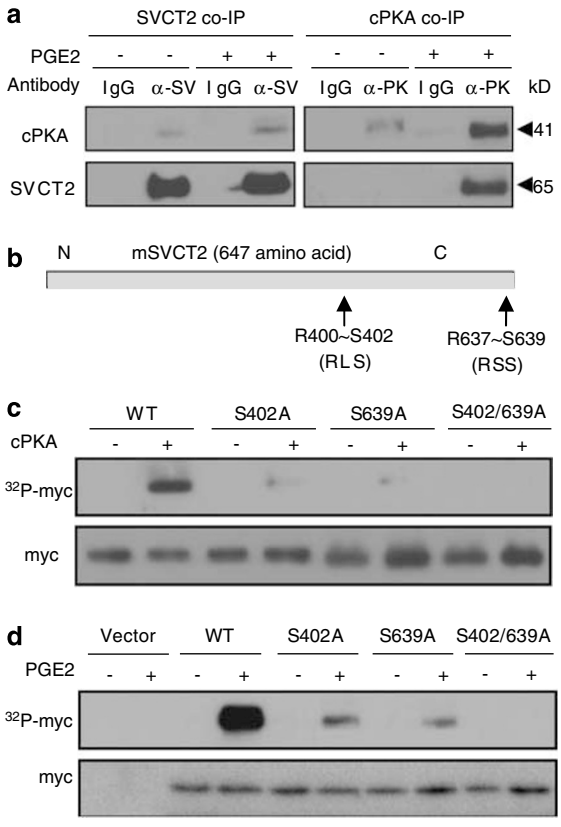

Figure 5 Physical interactions between PKA and SVCT2 and phosphorylation assays *in vitro*, and in intact cells. For co-immunoprecipitation, MC3T3-E1 cells were precultured in serum-free αMEM containing 1 μg/ml of indomethacin for 3 h, and further treated along with or without PGE2 for 1 h. After treatment, whole cell lysis was harvested, and the proteins were immunoprecipitated with normal serum IgG, SVCT2 (α-SV) or cPKA (α-PK) antibodies followed by SDS-PAGE and Western blotting for detection of cPKA and SVCT2 antigen (**a**). Putative phosphorylation sites for PKA in SVCT2 were shown (**b**). For *in vitro* phosphorylation assay, cells were transiently transfected with myc-tagged SVCT2 or its variants, and the myc-tagged proteins were purified by anti-myc-agarose beads, and subjected to a kinase reaction with [γ-^{32}P]ATP catalyzed with (+) or without (−) the purified catalytic subunit of PKA (cPKA). Whole kinase reactions (**c**) were subjected to electrophoresis, followed by autoradiography (upper bands) and Western blotting with myc-antibody (lower bands). For phosphorylation assay of SVCT2 in intact cells, MC3T3-E1 cells were transfected with empty vector, myc-tagged SVCT2 or the corresponding variants, 2 days after transfection, cells were cultured in a phosphate-free medium containing 0.25 mci/ml of [^{32}P]orthophosphate, followed by stimulation with 1 μM PGE2 for 1 h. The proteins were immunoprecipitated with myc antibody followed by electrophoresis, autoradiography (upper bands), and Western blotting with myc antibody (lower bands) (**d**). Experiments were independently duplicated, and results were qualitatively identical. Representative experiments are shown

bands corresponded to the SVCT2 variants, and similar levels of myc-tagged SVCT2 variants were present among the various immunoprecipitates (Figure 5c).

To confirm that S402 and S639 are phosphorylated in intact cells responding to PGE2, we performed *in vivo* phosphorylation assays. Under basal conditions, no significant phosphorylation was detected for any of the SVCT2 variants. However, upon PGE2 stimulation, the wild-type SVCT2 became highly phosphorylated (Figure 5d), both S402A and S639A largely reduced phosphorylation and S402/639A completely abolished phosphorylation in response to PGE2 (Figure 5d). Western blotting using the myc antibody revealed similar levels of myc-SVCT2 variants among the immunoprecipitates, indicating that the different variants were expressed at similar levels (Figure 5d). Together, these data convincingly demonstrate that SVCT2 can be phosphorylated by PKA at Ser402 and Ser639 sites both *in vitro* and in intact cells.

Ser402 and Ser639 are critical for SVCT2 plasma membrane localization. To understand the contribution of SVCT2 phosphorylation by PKA, we performed transient transfection with myc-tagged SVCT2 variants and immunostaining to examine the subcellular localization of myc-tagged SVCT2 variants by using a myc antibody. MC3T3-E1 cells were transfected with pCS2-MT-SVCT2, pCS2-MT-SVCT2^{S402A} pCS2-MT-SVCT2^{S639A} or pCS2-MT-SVCT2$^{S402/639A}$ expression vector, after transfection, cells were stimulated with 1 μM of PGE2 for 1 h, and the subcellular localization of myc-tagged proteins were detected by mouse anti-myc first antibody and anti-mouse Alex555 second antibody under confocal microscopy. Without PGE2 stimulation, myc-tagged wide-type SVCT2 was distributed diffusely in the cytoplasm (Figure 6a); however, under stimulation of PGE2, myc-tagged wide-type SVCT2 was mainly detected in the portion of plasma membrane (Figure 6b). In contrast, even though stimulation of PGE2, the myc-tagged SVCT2^{S402A} (Figure 6c), SVCT2^{S639A} (Figure 6d), and SVCT2$^{S402/639A}$ (Figure 6e) were detected mainly in the cytoplasm instead of plasma membrane. Thus, phosphorylation of Ser402 and Ser639 sites is required for PGE2-driven SVCT2 plasma membrane localization.

Discussion

The present study describes four novel findings. (i) PGE2 induces osteoblast-like differentiation partially through induction of SVCT2-mediated AA uptake. (ii) PGE2-induced plasma membrane translocation of SVCT2 results in the increase of AA uptake. (iii) Activation of EP4 receptor and PKA is required in PGE2-associated effects. (iv) Phosphorylation of SVCT2 at Ser402 and Ser639 sites by PKA promotes plasma membrane translocation of SVCT2 in MC3T3-E1 cells.

PGE2 is among the most important local factors with autocrine/paracrine roles in the bone.[28] PGE2 treatment for different times stimulates not only early-stage differential markers including ALP and collagen expression but also late-stage marker, OCN expression, and mineralization, which correspond to previous reports indicating that PGE2 induces ALP activity and collagen synthesis[21,22] as well as OCN expression[29] and mineralization.[23,24] The same effects of PGE2 were observed in primary calvarial culture system, suggesting that PGE2 plays an important role in bone formation. Although Kajii *et al*. reported that indomethacin induces ALP activity, collagen synthesis, and mineralization in MC3T3-E1 cells, in our system, we added 1 μg/ml of indomethacin to inhibit completely endogenous PGE2 production from MC3T3-E1 cells both in vehicle- and PGE2-containing medium;[30] therefore, the abovementioned effects

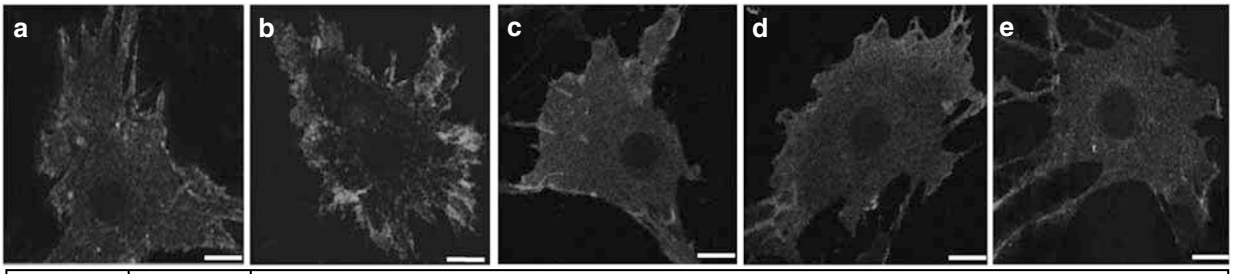

Figure 6 Indirect immunostaining for subcellular localization of myc-tagged SVCT2 and its variants in MC3T3-E1 cells in response to PGE2. MC3T3-E1 cells were plated at an initial density of 3000 cells/cm^2 and cultured in complete αMEM medium, after 24 h, cells were transiently transfected with each 0.1 μg/cm^2 of myc-tagged pCS2-MT-SVCT2 (WT), pCS2-MT-SVCT2^{S402A} (S402A), pCS2-MT-SVCT2^{S639A} (S639A) or double mutant pCS2-MT-SVCT2$^{S402/639A}$ (S402/639A) expression vector by lipofectamine. Then, cells were precultured in serum-free αMEM containing 1 μg/ml of indomethacin for 3 h, and then treated along with 1 μM PGE2 for additional 1 h. Immunostaining was performed by using mouse anti-myc first antibody and anti-mouse Alex555-conjugated second antibody. Stained cells were examined under an Olympus confocal microscope (bars, 100 μm)

of PGE2 are derived from exogenous PGE2 rather than indomethacin and endogenous PGE2. It is well documented that indomethacin inhibits PGE2 production through non-selective inhibition of cyclo-oxygenase (COX) in MC3T3-E1 cells,[31] our results indicate that PGE2 obviously induces osteoblast-like differentiation, suggesting that induction of osteoblast-like differentiation by indomethacin may have resulted from inhibition of COX-2 rather than from inhibition of PGE2 production, and this notion was further supported by previous report.[32]

We previously found that overexpression of SVCT2 and consequent increase of AA uptake into MC3T3-E1 cells lead to induction of osteoblast-like differentiation,[12] implying that any factor able to increase AA uptake into MC3T3-E1 cells might result in stimulation of osteoblast-like differentiation. In this study, we reveal that PGE2 stimulates AA uptake with increases in V_{max} and no change in K_m, indicating that PGE2 stimulates AA incorporation by increasing SVCT2 activity rather than increasing the affinity to SVCT2, which corresponds to our another finding that PGE2 induces AA uptake through increase of SVCT2 localization in plasma membrane instead of induction of SVCT2 mRNA or protein expression in MC3T3-E1 cells. Additionally, we first cloned mouse dnSVCT2 cDNA and indicate that overexpression of dnSVCT2 functionally leads to decreases of V_{max} but not K_m value in AA uptake and no effect on endogenous SVCT2 levels, consistent with previous report that human dnSVCT2 gives rise to a nonfunctional transport and acts as a dominant-negative mutant in AA uptake.[25] Overexpression of dnSVCT2 decreases the basal levels of ALP, collagen, OCN expression, and mineralization, corresponding to our previous findings that overexpression of SVCT2 stimulates osteoblast-like differentiation,[12] and Ca^{2+}, PO_4^{3-}, or Zn^{2+} enhances osteoblast-like differentiation through increase of SVCT2 expression and AA uptake into MC3T3-E1 cells.[10,11] In addition to decreasing the basal levels of osteoblast differential markers expression and mineralization, dnSVCT2 also marvelously attenuates PGE2-induced differential markers including ALP, collagen, and OCN expression as well as mineralization, providing the evidence that SVCT2 and AA uptake mediate PGE2-induced osteoblast-like differentiation.

Moreover, PGE2 neither induces SVCT2 mRNA expression nor increases SVCT2 protein levels in whole cells, implying that PGE2-induced AA uptake is not resulted from upregulation of SVCT2 expression in MC3T3-E1 cells. Furthermore, Western blotting results indicate that PGE2 time- and dose-dependently increases SVCT2 levels in plasma membrane, and concurrently decreases SVCT2 levels in cytoplasm, which is consistent with the immunostaining results indicating that PGE2 drives SVCT2 to plasma membrane from cytoplasm without obvious change of SVCT2 protein levels in whole MC3T3-E1 cells. Among various transporters, it is common that they exert their functions through subcellular redistribution. Insulin stimulates glucose uptake in adipocytes, skeletal, and cardiac muscles by promoting the subcellular redistribution of GLUT4, one of oxidative vitamin C transporter also serving as a facilitative glucose transporter, from an intracellular compartment (GLUT4 storage vesicle) to the plasma membrane.[33–35] For hSVCT1, decrease in AA uptake in COS-1 cells treated with PKC inhibitor is associated with a redistribution of hSVCT1 from the cell surface to intracellular membranes.[36]

EP1 receptor inhibitor, AH-6809, does not affect PGE2-induced SVCT2 translocation, AA uptake, osteoblast differential markers expression, and mineralization, suggesting that PGE2-associated effects are not due to activation of EP1 receptor subtype. However, EP4 receptor inhibitor, AH-23848B abrogates PGE2-associated effects, suggesting that activation of EP4 subtype and subsequent increase of cAMP contents are involved in PGE2-associated effects. PGE2-induced elevation of cAMP through EP4 receptor results in an increase in PKA activity in various cell types,[37] thus, cAMP-dependent PKA activation might play a key role in PGE2-associated effects in MC3T3-E1 cells. This notion is further supported by our findings that H-89, a PKA inhibitor, reduces PGE2-induced ALP activity, Hyp contents, AA uptake, and SVCT2 membrane translocation.

Putative membrane topology analysis of rat SVCT1 and SVCT2 predicated five potential sites for protein kinase C-dependent phosphorylation. Additional cAMP-dependent phosphorylation sites are present in the C-terminal of SVCT1 and SVCT2.[5,38] Activation of PKC has been shown to inhibit

Na^+-dependent vitamin C transport in a cell line derived from rabbit nonpigmented ciliary epithelium and in oocytes expressing hSVCT1 and hSVCT2.[6,39] PKC activator phorbol 12-myristate 13-acetate (PMA) causes a time- and concentration-dependent decrease in AA transport activity in COS-1 cells, for hSVCT1 but not hSVCT2,[36] the decrease in AA uptake is correlated with a redistribution of the transporter from the cell surface to intracellular membranes. In our case, the immunocomplexes precipitated by SVCT2 antibody contain cPKA under stimulation with PGE2 or without PGE2 indicating that the specifically physical interaction between SVCT2 and cPKA is PGE2-independent, however, the immunocomplexes precipitated by cPKA antibody contain SVCT2 only after exposure to PGE2 suggesting PGE2-dependent interaction between SVCT2 and cPKA. This discrepancy might be due to the antibody issue or other molecules existing in the complexes. Thus, PGE2 signaling does not appear to control PKA and SVCT2 complex formation, but may instead phosphorylate SVCT2 by PKA within the complex.

Recent report demonstrated that PGE2, through PKA activation, promotes β-catenin signaling in colon cancer cells, and the promoting effect of PKA is attributed to phosphorylation and inactivation of GSK3.[40] In mouse SVCT2, two putative PKA phosphorylation consensus sites residing in the fifth intracellular loop between transmembrane domain 10 and transmembrane domain 11 (Ser402) and in C-terminal (Ser639), respectively, this two putative sites were hydrophilic as predicated by topology assay. Our present finding reveals that in PKA–SVCT2 complex, SVCT2 serves as a substrate of PKA, and PKA activation by PGE2 phosphorylates SVCT2 at both Ser402 and Ser639 sites of SVCT2 protein, this finding was not reported previously. As S402A, S639A, and double mutation surely attenuate the phosphorylation of SVCT2, we propose one potential mechanism wherein phosphorylation of SVCT2 by PKA at Ser402 and Ser639 sites promotes the plasma membrane translocation of SVCT2, thereby, our data indicated that S402A and S639A mutations nearly abolish SVCT2 plasma membrane translocation under stimulation of PGE2, supporting this notion that phosphorylation of SVCT2 at Ser402 and Ser639 sites is required for PGE2-induced SVCT2 plasma membrane translocation. However, why the phosphorylated SVCT2 is subjected to plasma membrane translocation is not understood and is worth further study in future.

In summary, by using biochemical and molecular biological approaches the present study has uncovered a signaling cascade that operates in conjunction with PGE2-induced SVCT2 plasma membrane localization to osteoblast-like differentiation (Figure 7). In this cascade, PGE2 signals activate PKA through EP4 receptor and most likely AC and cAMP. As a result, cytoplasm SVCT2 is phosphorylated by PKA at Ser402 and Ser639 sites and thereby localized to the plasma membrane to facilitate AA uptake into cells, which further leads to promotion of osteoblast-like differentiation in MC3T3-E1 cells.

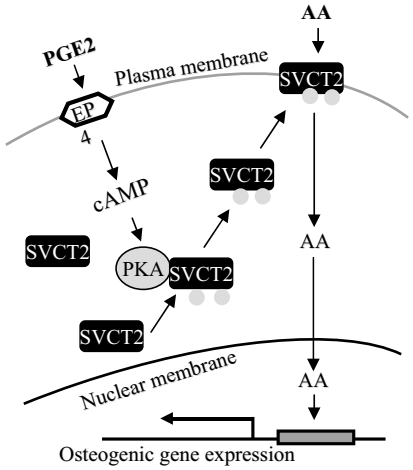

Figure 7 A model for PGE2 stimulating osteoblast-like differentiation in MC3T3-E1 cells through induction of SVCT2 plasma membrane localization and AA uptake which is resulted from activation of EP4-AC-cAMP-PKA signaling cascade and subsequent phosphorylation of SVCT2 at Ser402 and Ser639 sites by PKA

Materials and Methods

Plasmid constructions. The full-length of murine SVCT2 cDNA was amplified by PCR as described previously,[9] and cloned into 6 × myc-epitope-tagged expression vector, pCS2-MT at *Xba*I site, named pCS2-MT-SVCT2. Point mutants at the putative PKA phosphorylation sites of SVCT2, named pCS2-MT-$SVCT2^{S402A}$, pCS2-MT-$SVCT2^{S639A}$, and pCS2-MT-$SVCT2^{S402/609A}$ were generated by using pCS2-MT-SVCT2 and appropriate oligonucleotides with the Stratagene QuickChange site-directed mutagenesis method (Stratagene, Cedar Creek, TX, USA). All these plasmids were confirmed by sequencing. For cloning SVCT2 short isoform (dnSVCT2), cDNA from MC3T3-E1 cells (ATCC, Rockville, MD, USA) was used as a template for PCR-cloning of mouse dnSVCT2, and oligonucleotide primers were arranged as follows: 5′-GTCTTGATGA TGGGTATCGG-3′ (sense) and 5′-CTATACTGTGGCCTGGGAAT-3′ (antisense). The PCR products contained ∼2 kb (SVCT2 full-length cDNA) and ∼1.6 kb (dnSVCT2) length fragments, and the short fragment was cloned into the retroviral expression vector, pLXRN (Clontech Laboratories Inc., Mountain View, CA, USA) at *Sal*I and *Avr*II sites, the construct named pLXRN-dnSVCT2 was verified by a DNA sequencer. Moreover, EGFP cDNA was subcloned into pLXRN to form the construct named pLXRN-EGFP as a control expression vector.

Cell culture and treatment. MC3T3-E1 cells were maintained in α-modification of Eagle's medium (αMEM, ICN Biomedicals Co, Aurora, OH, USA) containing 50 mg/l of AA and 10% fetal calf serum in 5% CO_2 at 37°C. For PGE2 (Cayman Chemicals, Ann Arbor, MI, USA) treatment, cells were previously exposed in serum-free αMEN medium containing 1 μg/ml of indomethacin (Nakalai Tesque, Kyoto, Japan) for 3 h and further treated along with the indicated concentrations of PGE2, indomethacin was used for inhibition of endogenous PGE2 production. For treatment of inhibitors, cells were treated with 6-isopropoxy-9-oxoxanthine-2-carboxylic acid (AH 6809, EP1 inhibitor, Cayman Chemicals, Ann Arbor, MI, USA), [1(*Z*),2,5]-(±)-7-[5-[[(1,1′-biphenyl)-4-yl-methoxy]-3-hydroxy-2-(1-piperidinyl) cyclopentyl]-4-heptanoic acid] (AH-23848B, EP4 inhibitor, Cayman Chemicals), or *N*-[2-(p-Bromocinamylamino) ethyl]-5-isoquinolinesulfonamide dihydrocholoride (H-89, PKA inhibitor, Sigma, St Louis, MO, USA) along with indomethacin 3 h before further treatment of indicated concentration of PGE2. For mineralization experiments, cells were treated with PGE2 along with 1 μg/ml of indomethacin for indicated times in the presence of 50 mg/l AA and 5 mM β-glycerophosphate (Sigma).

ALP activity, Hyp content measurement and von Kossa staining. Determination of ALP activity was performed as described previously,[12] and the activity was expressed as nanomoles of p-nitrophenol formed per minute per milligram of protein. Hyp contents were evaluated by Woessner's method[13] and were expressed as $\mu g/10^5$ cells. von Kossa's staining was processed to monitor the mineralized nodules by using 5% silver nitrate, as described previously.[12]

Northern blotting. Total RNA was isolated using Sepasol-RNA II Super (Nakalai Tesque) by the acid guanidine–phenol–chloroform method. RNA (10 μg per lane) was loaded onto a 1% agarose gel, transferred to a Hybond-XL membrane (Amersham-Pharmacia, Piscataway, NJ, USA) and crosslinked by UV irradiation. cDNA fragments of SVCT2 (nt 1099–1495, GenBank Accession No. NM_018824) was labeled with [α-^{32}P]dCTP (0.295 MBq/lmol, Perkin–Elmer Life Science, Boston, MA, USA) and hybridized with the blots. Messenger RNA signals were detected and analyzed by using the BAS 1500 Mac radioimaging system (Fuji Film, Tokyo, Japan). All membranes were reprobed with a ^{32}P-labeled DNA probe for mouse 18S rRNA as an internal control.

[l-^{14}C]AA uptake. The uptake assay was described previously.[10,11] Briefly, after a rinse with incubation buffer (in mM: 140 NaCl, 4.2 $KHCO_3$, 5.8 KCl, 1.3 $CaCl_2$, 0.5 $MgCl_2$, 10 HEPES, and 1 dithiothreitol, pH 7.4), cells were incubated with 6.25, 12.5, 25, 50 or 100 μM (for kinetic parameter assays) or 25 μM (for single dose uptake assays) [l-^{14}C]AA (Perkin–Elmer Life Science) at 37°C for 30 min, and the incorporated radioactivity was measured with a liquid scintillation counter. Kinetic constants of transport, the apparent Michaelis–Menten constant (K_m) and the maximal rate of AA uptake (V_{max}) were calculated from specifically incorporated radioactivity with various concentrations of AA by fitting data to a double reciprocal plot. Specific uptake was calculated as the total incorporated radioactivity in the absence of cold AA minus the nonspecific radioactivity in excessive cold AA (10 mM). AA uptake appeared to increase linearly within 1 h under these experimental conditions.

Retroviral gene expression system. GP293 retroviral packaging cells (Clontech) were maintained in Dulbecco's modified Eagle medium containing 10% FCS. Cells were transiently cotransfected with 4 μg of pVSV-G vector (Clontech) plus 5 μg of either pLXRN-dnSVCT2 or pLXRN-EGFP by the lipofectamin (Invitrogen). After transfection, medium was changed to regular medium, and retrovirus-containing supernatants were harvested 48 h after transfection, virus was concentrated by ultracentrifugation according to the manufacturer's protocol, and the retroviral supernatants with titer more than 1×10^6 cfu/ml were used for infection. MC3T3-E1 cells were exposed to retrovirus containing medium for 24 h in the presence of 6 μg/ml of polybrene (Nacalai Tesque), and the infection efficiency was determined by EGFP-positive cells (more than 90%). After infection, virus-containing medium was changed to desired experimental condition for assessment of dnSVCT2 and SVCT2 protein expression, AA uptake, ALP activity, Hyp contents, OCN expression, and mineralization in either dnSVCT2 or EGFP expressing virus-infected MC3T3-E1 cells with or without PGE2 stimulation.

Subcellular fractions and Western blotting. For preparation of whole cell lysis, cells were washed twice with ice-cold phosphate-buffered saline (PBS), harvested and transferred to lysis buffer containing 25 mM Tris–HCl (pH 7.5), 150 mM NaCl, 5 mM $MgCl_2$, 1% NP-40, 1 mM DTT, and 5% glycerol and further incubated at 4°C for 20 min, then, mixture was centrifuged at 12 000 $\times$ g for 30 min, and supernatant was used as whole cell lysis for Western blotting. For preparation of subcellular fractions, cells were rinsed twice with PBS and harvested, then, cells were homogenized in 0.6 ml of ice-cold homogenization buffer A (10 mM HEPES–KOH, pH 7.2, 0.25 M sucrose) containing a complete protease inhibitor mixture (Roche Diagnostics) by a glass Dounce homogenizer, and centrifuged at 2500 r.p.m. for 10 min at 4°C to remove nuclei and unbroken cells. The postnuclear supernatant was then centrifuged at 120 000 $\times$ *g* for 60 min at 4°C to obtain cytosol and membrane fractions. The supernatant was used as a cytosol fraction, and the pellet was further rinsed with homogenization buffer A twice, dissolved in lysis buffer (50 mM Tris-HCl, pH 7.5, 1% Triton X-100, 2.5 mM EDTA, 0.25 M NaCl), and centrifuged at 12 000 r.p.m. for 10 min at 4°C, the supernatant was used as a membrane fraction. Western blotting was described previously,[11,12] briefly, protein samples were separated by 10% SDS-PAGE and transferred to a polyvinylidene difluoride membrane (Millipore, Billerica, MA, USA). Antigens on the membrane were first probed with desired first antibody including rabbit anti-SVCT2 antibody[11] and mouse anti-OCN antibody (SC-1822, Santa Cruz Biotechnology Inc., Santa Cruz, CA, USA) and then horse peroxidase-conjugated anti-rabbit or anti-mouse secondary antibody (Santa Cruz Biotechnology). The immunoreactive bands were visualized by enhanced ECL system (Amersham-Pharmacia).

Immunostaining of endogenous SVCT2 and myc-tagged SVCT2. To determine the effect of PGE2 and inhibitors on subcellular localization of endogenous SVCT2, cells seeded at 0.75×10^4/cm^2 were cultured overnight in regular medium, and directly switched to the serum-free medium for 24 h, then, cells were pretreated with inhibitors for 3 h, and further treated along with PGE2 (1 μM) for 1 h. To examine the effect of PGE2 on subcellular localization of myc-tagged SVCT2, cells were transfected with proper amount of pCS2-MT-SVCT2, pCS2-MT-SVCT2^{S402A}, pCS2-MT-SVCT2^{S639A} or pCS2-MT-SVCT2$^{S402/639A}$ expression vector, after transfection, cells were cultured in regular medium for 24 h, starved for additional 24 h, and further treated with 1 μM PGE2 for 1 h. For immunostaining, cells were fixed in PBS-buffered 3.7% formaldehyde containing 30 mM sucrose for 10 min, neutralized in 50 mM NH_4Cl for 10 min, before permeabilized with 0.1% Triton X-100/PBS for 30 min. After blocking in 1% BSA plus 1% normal sheep serum, the cells were then incubated with anti-rabbit SVCT2 or anti-mouse myc primary antibody (Santa Cruz) for 60 min, washed in 0.1% Triton X-100/PBS, and finally incubated with anti-rabbit or anti-mouse Alexa555-conjugated secondary antibody (Invitrogen). As controls for specificity, some cells were stained with the secondary antibody only. All procedures were performed at room temperature. Stained cells were examined under an Olympus confocal microscope.

Immunoprecipitation. The lysates from PGE2-treated or transfected MC3T3-E1 cells were used for immunoprecipitation. The cells were washed twice with ice-cold PBS and lysed in the extraction buffer (300 μl/10^6 cells) containing 150 mM NaCl, 25 mM HEPES (pH 7.4), 0.5% Nonidet P-40, 2 mM EDTA, 2 mM EGTA, 100 μM orthovanadate, and protease inhibitor cocktail. The lysates were cleared by centrifugation at 15 000 $\times$ g for 10 min, and the immunoprecipitation of endogenous PKA and SVCT2 was performed by using rabbit anti-cPKA (Santa Cruz) and rabbit anti-SVCT2 antibodies, respectively. While the immunoprecipitation for MC3T3-E1 cells transfected with pCS2-MT-SVCT2, pCS2-MT-SVCT2^{S402A}, pCS2-MT-SVCT2^{S639A} or pCS2-MT-SVCT2$^{S402/639A}$ expression vector was performed by using mouse anti-myc antibody. At the same time, immunoprecipitates with normal nonimmune IgG serum instead of specific antibody were used as an internal negative control. Immunoprecipitations were performed by overnight incubation of the cleared protein A-conjugated agarose beads followed by four times washes with 1 ml of lysis buffer. The PKA and SVCT2 immune complex was boiled in 2 $\times$ sample buffer and subjected to Western blotting with the desired antibody. Myc-tagged SVCT2 and its mutants immune complex was subjected to phosphorylation assay *in vitro* and in intact cells.

***In Vitro* ^{32}P labeling of SVCT2.** MC3T3-E1 cells were transfected with proper amount of pCS2-MT-SVCT2, pCS2-MT-SVCT2^{S402A} pCS2-MT-SVCT2^{S639A} or pCS2-MT-SVCT2$^{S402/639A}$ expression vector, after transfection, cells were cultured in regular medium for 24 h, then, cells were starved for an additional 24 h, and further stimulated with 1 μM PGE2 for 1 h. The myc-tagged protein were purified by anti-myc-agarose beads, the beads were washed once with PKA assay buffer (20 mM Tris–HCl (pH 7.4), 100 mM NaCl, 10 mM $MgCl_2$, 1 mM ATP), and then incubated with 45 μl of PKA assay buffer supplemented with 0.1 mM dithiothreitol, five units of purified protein kinase A catalytic subunit (Promega, Madison, WI, USA), and 5 μCi of [γ-^{32}P]ATP (Perkin–Elmer) at 30°C for 30 min. The reaction was stopped by the addition of 15 μl of 4 $\times$ sample buffer and boiling for 5 min. Proteins were subjected to SDS-PAGE, followed by autoradiography and Western blotting with anti-myc antibody.

^{32}P labeling of SVCT2 in intact cells. MC3T3-E1 cells were transfected with proper amount of pCS2-MT, pCS2-MT-SVCT2, pCS2-MT-SVCT2^{S402A}, pCS2-MT-SVCT2^{S639A} or pCS2-MT-SVCT2$^{S402/639A}$ expression vector, after transfection, cells was cultured in regular medium for 24 h, and starved for additional 24 h. Then, cells were incubated with 0.25 mCi/ml [^{32}P]orthophosphate (Perkin–Elmer) in both phosphate- and serum-free medium for 3 h, followed by three washes and stimulation with 1 μM of PGE2 for 1 h. Cells were then lysated, and the lysis was subjected to immunoprecipitation with myc antibody as described above, followed by electrophoresis, autoradiography, and Western blotting with myc antibody.

Statistical analysis. Numerical data were expressed as means $\pm$ S.D. and analyzed by ANOVA and Tukey–Kramer multiple comparisons test. Statistical significance was assessed at levels of $P < 0.05$ and $P < 0.01$. Experiments were independently triplicated and results were qualitatively identical. Representative experiments are shown.

Acknowledgements. X Wu received a postdoctoral fellowship from the Society of Japanese Pharmacopoeia. We thank Drs K Tanaka, N Itoh, and T Nakanishi from Osaka University for valuable advice and Dr MJ Hilton from Washington University in St Louis for discussion of this work, and correcting errors of grammars.

1. Franceschi RT. The role of ascorbic acid in mesenchymal differentiation. *Nutr Rev* 1992; **50**: 65–70.
2. Franceschi RT, Iyer BS, Cui Y. Effect of ascorbic acid on collagen matrix formation and osteoblast differentiation in murine MC3T3-E1 cells. *J Bone Miner Res* 1994; **9**: 843–854.
3. Franceschi RT, Iyer BS. Relationship between collagen synthesis and expression of the osteoblast phenotype in MC3T3-E1 cells. *J Bone Miner Res* 1992; **7**: 235–246.
4. Shi S, Kirk M, Kahn AJ. The role of type I collagen in the regulation of osteoblast phenotype. *J Bone Miner Res* 1996; **11**: 1139–1145.
5. Tsukaguchi H, Tokui T, Mackenzie B, Berger UV, Chen X-Z, Wang Y *et al.* A family of mammalian Na+-dependent L-ascorbic acid transporters. *Nature* 1999; **399**: 70–75.
6. Daruwala R, Song J, Koh WS, Rumsey SC, Levine M. Cloning and functional characterization of the human sodium-dependent vitamin C transporters hSVCT1 and hSVCT2. *FEBS Lett* 1999; **460**: 480–484.
7. Sotiriou S, Gispert S, Cheng J, Wang Y, Chen A, Hoogstraten-Miller S *et al.* Ascorbic-acid transporter Slc23a1 is essential for vitamin C transport into brain and for perinatal survival. *Nat Med* 2002; **8**: 514–517.
8. Franceschi RT, Wilson JX, Dixon SJ. Requirement for Na^+-dependent ascorbic acid transport in osteoblast function. *Am J Physiol* 1995; **268**: C1430–C1439.
9. Fujita I, Hirano J, Itoh N, Nakanishi T, Tanaka K. Dexamethasone induces sodium-dependent vitamin C transporter in a mouse osteoblastic cell line MC3T3-E1. *Br J Nutr* 2001; **86**: 145–149.
10. Wu X, Itoh N, Taniguchi T, Nakanishi T, Tanaka K. Requirement of calcium and phosphate ions in expression of sodium-dependent vitamin C transporter 2 and osteopontin in MC3T3-E1 osteoblastic cells. *Biochim Biophys Acta* 2003; **1641**: 65–70.
11. Wu X, Itoh N, Taniguchi T, Nakanishi T, Tatsu Y, Yumoto N *et al.* Zinc-induced sodium-dependent vitamin C transporter 2 expression: potent roles in osteoblast differentiation. *Arch Biochem Biophys* 2003; **420**: 114–120.
12. Wu X, Itoh N, Taniguchi T, Hirano J, Nakanishi T, Tanaka K. Stimulation of differentiation in sodium-dependent vitamin C transporter 2 overexpressing MC3T3-E1 osteoblasts. *Biochem Biophys Res Commun* 2004; **317**: 1159–1164.
13. Harada S, Nagy JA, Sullivan KA, Thomas KA, Endo N, Rodan GA *et al.* Induction of vascular endothelial growth factor expression by prostaglandin E2 and E1 in osteoblasts. *J Clin Invest* 1994; **93**: 2490–2496.
14. Klein DC, Raisz LG. Prostaglandin: stimulation of bone resorption in tissue culture. *Endocrinology* 1970; **86**: 1436–1440.
15. Santoro MG, Jaffe BM, Simmons DJ. Bone resorption *in vitro* and *in vivo* in PGE-treated mice. *Proc Soc Exp Biol Med* 1977; **156**: 373–377.
16. Yang R-S, Liu T-K, Shiau S-Y. Increased bone growth by local prostaglandin E2 in rats. *Calcif Tissue Int* 1993; **52**: 57–61.
17. Mori S, Jee WSS, Li XJ, Chan S, Kimmel DB. Effects of prostaglandin E2 on production of new cancellous bone in the axial skeleton of ovariectomized rats. *Bone (Elmsford)* 1990; **11**: 103–113.
18. Chyun YS, Raisz LG. Stimulation of bone formation by prostaglandin E2. *Prostaglandins* 1984; **27**: 97–103.
19. Woodiel FN, Fall PM, Raisz LG. Anabolic effects of prostaglandins in culture fetal rat calvariae: structure-activity relations and signal transduction pathway. *J Bone Miner Res* 1996; **11**: 1249–1255.
20. Yang RS, Fu WM, Wang SM, Lu KS, Liu TK, Lin-Shiau SY. Prostaglandin-induced morphological changes in osteoblasts. *Bone* 1998; **22**: 629–636.
21. Hakeda Y, Nakatani Y, Hiramatsu M, Kurihara N, Tsunoi M, Ikeda E *et al.* Inductive effects of prostaglandins on alkaline phosphatase in osteo-blastic cells, clone MC3T3-E1. *J Biochem* 1985; **97**: 97–104.
22. Hakeda Y, Nakatani Y, Kurihara N, Ikeda E, Maeda N, Kumegawa M. Prostaglandin E2 stimulates collagen and non-collagen protein synthesis and prolyl hydroxylase activity in osteoblastic clone MC3T3-E1 cells. *Biochem Biophys Res Commun* 1985; **126**: 340–345.
23. Nagata T, Kaho K, Nishikawa S, Shinohara H, Wakano Y, Ishida H. Effect of prostaglandin E2 on mineralization of bone nodules formed by fetal rat calvarial cells. *Calcif Tissue Int* 1994; **55**: 451–457.
24. Flanagan AM, Chambers TJ. Stimulation of bone nodule formation *in vitro* by prostaglandin E1 and E2. *Endocrinology* 1992; **130**: 443–448.
25. Lutsenko EA, Carcamo JM, Golde DW. A human sodium-dependent vitamin C transporter 2 isoform acts as a dominant negative inhibitor of ascorbic acid transport. *Mol Cell Biol* 2004; **24**: 3150–3156.
26. Suzawa T, Miyaura C, Inada M, Maruyama T, Sigimoto Y, Ushikubi F *et al.* The role of prostaglandin E receptor subtypes (EP1, EP2, EP3 and EP4) in bone resorption: an analysis using specific agonist for the respective EPs. *Endocrinology* 2000; **141**: 1554–1559.
27. Suda M, Tanaka K, Natsui T, Usui T, Tanaka I, Fukushima M *et al.* Peostaglandin E receptor subtypes in mouse osteoblastic cell line. *Endocrinology* 1996; **137**: 1689–1705.
28. Hakeda Y, Yoshino T, Nakatani Y, Kurihara N, Maeda N, Kumegawa M. Prostaglandin E2 stimulates DNA synthesis by a cAMP-independent pathway in osteobalst clone MC3T3-E1 cells. *J Cell Physiol* 1986; **128**: 155–161.
29. Conconi MT, Tommasini M, Baiguera S, Coppi PD, Parnigotto PP, Nussdorfer GG. Effects of prostaglandin E1 and E2 on the growth and differentiation of osteoblast-like cells cultured *in vitro*. *Int J Mol Med* 2002; **10**: 451–456.
30. Kajii T, Suzuki K, Yoshikawa M, Imai T, Matsumoto A, Nakamura S. Long-term effects of prostaglandin E2 on the mineralization of a clonal osteoblastic cell line (MC3T3-E1). *Arch Oral Biol* 1999; **44**: 233–241.
31. Tai H, Miyamura C, Philbeam CC, Tamura T, Ohsugi Y, Koishihara Y *et al.* Transcriptional induction of cyclooxygenase-2 in osteoblast is involved in interleukin-6 induced osteocalst formation. *Endocrinology* 1997; **138**: 2372–2379.
32. Ho ML, Chang JK, Chuang LY, Hsu HK, Wang GJ. Effect of nonsteroidal anti-inflammatory drugs and prostaglandins on osteoblastic functions. *Biochem Pharmacol* 1999; **58**: 983–990.
33. Rumsey SC, Daruwala R, Al-Hasani H, Zamowski MJ, Simpson IA, Levine M. Dehydroascorbic acid transport by GLUT4 in Xenopus oocytes and isolated rat adipocytes. *J Biol Chem* 2000; **275**: 28246–28253.
34. Bryant NJ, Govers R, James DE. Regulated transport of the glucose transporter GLUT4. *Nat Rev Mol Cell Biol* 2002; **3**: 267–277.
35. Watson RT, Kanzaki M, Pessin JE. Regulated membrane trafficking of the insulin-responsive glucose transporter 4 in adipocytes. *Endocr Rev* 2004; **25**: 177–204.
36. Liang WJ, Johnson D, Ma LS, Jarvis SM, Wei-Jun L. Regulation of the human vitamin C transporters expressed in COS-1 cells by protein kinase C. *Am J Physiol Cell Physiol* 2002; **283**: 1696–1704.
37. Fujino H, Salvi S, Regan JW. Differential regulation of phosphorylation of the cAMP response element-binding protein after activation of EP_2 and EP_4 prostanoid receptors by prostaglandin E_2. *Mol Pharmacol* 2005; **68**: 251–259.
38. Takanaga H, Mackenzie B, Hediger MA. Sodium-dependent ascorbic acid transporter family SLC23. *Pflugers Arch* 2004; **447**: 677–682.
39. Delamere NA, Coca-Prados M, Aggarwal S. Studies on regulation of the ascorbic acid transporter in a cell line derived from rabbit non-pigmented ciliary epithelium. *Biochim Biophys Acta* 1993; **1149**: 102–108.
40. Shao J, Jung C, Liu C, Sheng H. Prostaglandin E_2 stimulates the β-catenin/T cell factor-dependent transcription in colon cancer. *J Biol Chem* 2005; **280**: 26565–26572.

Supplementary Information accompanies the paper on Cell Death and Differentiation website (http://www.nature.com/cdd)